Multilayer perceptrons and conventional biosorption equations for modeling removal of Ni(II) by terrestrial moss

Bilge Özbay*

Environmental Engineering Department, University of Kocaeli, Izmit, Turkey, Tel. +90 262 3033202; Fax: +90 262 3033163;
email: bilgealyuz@yahoo.com

ABSTRACT

In this study, multilayer perceptrons (MLPs) and conventional isotherm equations were used to model bisorption of nickel using terrestrial moss. Characterization of the biosorbent was examined by scanning electron microscopy and Fourier transform infrared spectroscopy analyses. Batch biosorption tests were performed to examine the impacts of different experimental conditions. Thermodynamic calculations were made to evaluate the feasibility of the biosorption. All of the experimental data (total 86 data-sets) were used for MLP modeling purposes whereas equilibrium data were used in Langmuir, Freundlich, and Temkin models. Adsorption kinetic data were tested using pseudo-first-order and second-order kinetic models. Performances of the models were evaluated considering calculated R^2 and mean standard error (MSE) values. Related isotherm and kinetic parameters were also calculated for conventional biosorption equations. In multilayer perceptron (MLP) modeling studies, network architecture with three hidden layers provided highest prediction efficiency. Although both MLPs and conventional models are regarded to be useful, perceptron models are thought to provide more representative information as all factors are evaluated simultaneously.

Keywords: Biosorption; Multilayer perceptrons; Conventional biosorption equations; Modeling performance; Terrestrial moss

1. Introduction

Biosorption is a well-known equilibrium separation process and effectively used in removal of numerous pollutant species from wastewaters [1]. This treatment technique may also be regarded as economical and environmentally friendly if low-cost biosorbents are used in the process. Among the various low-cost adsorbent types, biosorbents have gained increasing attention in recent years due to their advantages such as high-treatment efficiency, lower operational costs, and reduced sludge volumes to be disposed [2]. Beside these, biosorbents are attractive since they are abundant and locally available biomasses [3]. There are numerous species of biosorbents occur in the nature ubiquitously [4].

In literature, various biosorbent types such as propagated biomass of bacteria, yeast, fungi, and leaf-based biomasses were found to be useful for removal of different pollutants [5]. Chitosan-immobilized brown alga *Laminaria japonica* was used to adsorb nickel ions from aqueous medium [6]. *Jatropha curcas* deoiled cake also provided sufficient biosorption efficiencies for removal of toxic metals [7]. In another study, baker's yeast provided uptake capacity of 52.6 and 25.0 mg/g for

methylene blue and rhodamine B, respectively [8]. Methylene blue removal has also been performed using jackfruit leaf powder [9], pineapple leaf powder [10], and phoenix tree leaf powder [11]. Leaf powder obtained from different plants was also used to uptake metal ions such as copper [12] and lead [13].

Similar to other wastewater treatment methods, efficiency of biosorption processes is highly affected by various factors such as pH of the solution, agitation period, concentration of the pollutant, as well as the type and the dosage of the used biosorbent. Because of numerous involving factors, biosorption becomes a complex physico-chemical process. Numerous time-consuming experimental tests are demanded for determination of optimum conditions. Furthermore, theoretical and empirical models are also required for better understanding and accurate predictions. At the beginning, various isotherm models were developed in order to examine the experimental data of equilibrium conditions in particular. Langmuir, Freundlich, Brunauer Emmett Teller, Dubinin–Radushkevich, Thomas, and Temkin are some of the well-known conventional isotherm models commonly used in biosorption studies for analysis of equilibrium sorption data. Each of these models has been based on different hypotheses about the sorption mechanism occurring at the specific biosorption surfaces. Additionally, various kinetic models have been used to evaluate the adsorption kinetic data.

In recent years, multivariate statistical models have been preferred to model biosorption data. Multilayer perceptron (MLP) models, exhibiting the superiority of modeling complex and non-linear problems, can be successfully used in adsorption modeling purposes [14]. MLPs provide sufficient modeling efficiencies considering all experimental data as a whole. By this way, impacts of all involved factors (pH, biosorbent dosage, temperature, etc.) can be evaluated together. MLP models can produce more accurate and representative predictions [15].

In this study, it was aimed to model biosorption behaviors of nickel, a recalcitrant heavy metal, using terrestrial moss. With this aim MLP models, conventional isotherm equations (Langmuir, Freundlich, Temkin), and kinetic models (pseudo-first-order and second-order kinetic models) were applied to experimental data. Efficiency of the models was evaluated considering calculated R^2 values and standard errors. Moreover, advantages and deficiencies of the used models were discussed in detail.

2. Materials and methods

2.1. Experimental studies

2.1.1. Collection and preparation of terrestrial moss

Sphagnum is classified in the division Bryophyta, class Musci. There are four major Musci kinds seen in Turkey: *Polytrichum*, *Hydnum*, *Mnium*, and *Sphagnum*. *Sphagnum* sp. can be distinguished from others considering the following properties [16]:

(1) *Sphagnum* sp. has ramified stem.
(2) There are several sporangiums (enclosures in which spores are formed) on the tip branches.
(3) Lateral branches are renewed annually and old ones produce peat as a result of decaying process.
(4) Finally, *Sphagnum* sp. prefers more humid conditions to inhabit.

In the study, *Sphagnum* sp. has been identified considering the mentioned distinguishing characteristics.

Biomass of terrestrial moss *Spaghnum* sp. was collected from terrestrial area in northern region of Kocaeli, Turkey. After collection, it was washed with tap water in order to remove unwanted materials such as silt, sand, etc. After this, the moss was also washed with deionized water three times to clean the remaining impurities. The cleaned biomass was inactivated by heating in the oven at 70°C for 48 h. The dried moss was ground and sieved through 1 mm pore sieve. The prepared biosorbent was stored in the desiccators.

2.1.2. Characterization of the biosorbent

The morphological properties of the biosorbent were analyzed using scanning electron microscopy (SEM, JEOL, JSM 6060). Elemental analysis of the biosorbent was carried out using Thermo Finnigan 1112 Series Flash EA device. Furthermore, functional groups present in the biomass were specified using Perkin-Elmer Spectrum One FTIR spectrometer.

2.1.3. Batch biosorption tests

Batch biosorption method was performed using NUVE ST 30 model shaking water bath. 1,000 mg/L nickel stock solution was prepared by dissolving required amount of $Ni(NO_3)_2 \cdot 6H_2O$ in 1L distilled water. Standard nickel solutions ranging between 20 and 180 mg/L were prepared by dilutions from the

stock solution. pH adjustments were made using 0.1 N HCl and 0.1 N NaOH, and pH of the samples was measured using Thermo Scientific Orion 3-Star Plus pH meter. All used chemicals were of analytical grade and purchased from Merck. Predetermined biomass amounts (0.02–1 g) were added into samples of 100 mL volume and batch biosorption tests were performed. Samples were taken from the shaker at the end of agitation periods and filtered in order to separate the biomass. Finally, remaining metal concentration was analyzed by Hach Lange DR 5000 UV spectrophotometer with cuvette tests of LCK 337 for Ni(II). Dimethylglyoxime method was used during the analyses. According to this method, in presence of an oxidizing agent, nickel ions react with dimethylglyoxime in an alkaline solution. During reactions, an orange–brown-colored complex has been formed. Results were measured at 466 nm.

Impacts of pH, biosorbent dosage, metal concentration, agitation time, agitation speed, and temperature have been determined by batch biosorption tests. The biosorbed heavy metal amount (q_e) per unit moss was calculated using equation given below:

$$q_e = \frac{(C_0 - C_e)/V}{m} \tag{1}$$

where q_e (mg/g) represents the equilibrium biosorption capacity, and C_e (mg/L) are the initial and equilibrium nickel concentrations, respectively, V (L) is the volume, and m (g) is moss dosage.

2.1.4. Desorption and regeneration studies

Biosorption studies can be complemented with desorption tests as desorption data provide valuable information about the recovery of the biosorbed metal and reuse of the biosorbent in subsequent loading and unloading cycles [17]. With this aim, batch desorption experiments were performed in the study after biosorption tests.

In desorption tests, the metal-loaded biomass was contacted with 20 ml of the elutants (deionized water and 0.05 N HNO$_3$) on the shaker at 200 rpm. Samples were taken from the shaker at the end of predetermined periods and biosorbent was separated by filtration. Similar to the biosorption experiments, released nickel concentrations were analyzed by the spectrophotometer.

Regeneration and reuse of the biosorbent were also investigated in the study. With this aim, the biomass was washed with deionized water until the pH of the washed water reached neutral levels. Regenerated biomass was dried and reused. The biosorption–elution–regeneration cycle was repeated three times in the study.

2.2. MLP models

MLP, also known as multilayer feed-forward networks, are among the most widely used neural network types. Due to superiority of modeling complex non-linear relations, they are commonly preferred in numerous fields with different purposes [15].

Briefly, MLP consists of multiple layers of interconnected neurons producing adequate and rapid responses (outputs) to new in formations (inputs). There are three basic layer groups within this system: input layer, hidden layers, and output layer (Fig. 1). MLPs run due to black-box method with the interaction of neurons, which are connected by weights. In the system, each neuron is connected to all other neurons present in the next and previous layer [18]. Neurons in the hidden layer receive the weighted input signals and transform them into outputs which are a function of the sum of the inputs.

Various transfer functions are used in order to determine the input–output behaviors. MLPs generally use log-sigmoid (Logsig) transfer function that produces outputs between 0 and 1, as the net input of the neuron goes from negative to positive infinity. Mathematical expression for this non-linear function is given below:

$$f(x) = \frac{1}{1 + e^{-x}} \tag{2}$$

All data were normalized in the range 0–1 considering the general procedure of MLP. After then, data were divided into two subsets at ratio of approximately 2:1 for training and model testing purposes, respectively.

In this work, the Neural Network Toolbox of Matlab was used for all MLP simulation purposes.

2.3. The used isotherm models

In the study, Langmuir, Freundlich, and Temkin isotherms were applied to equilibrium data as they are among the most widely used conventional isotherm models.

2.3.1. Langmuir isotherm equation

The Langmuir isotherm is commonly used to model biosorption equilibrium and it assumes that maximum biosorption occurs at specific homogeneous
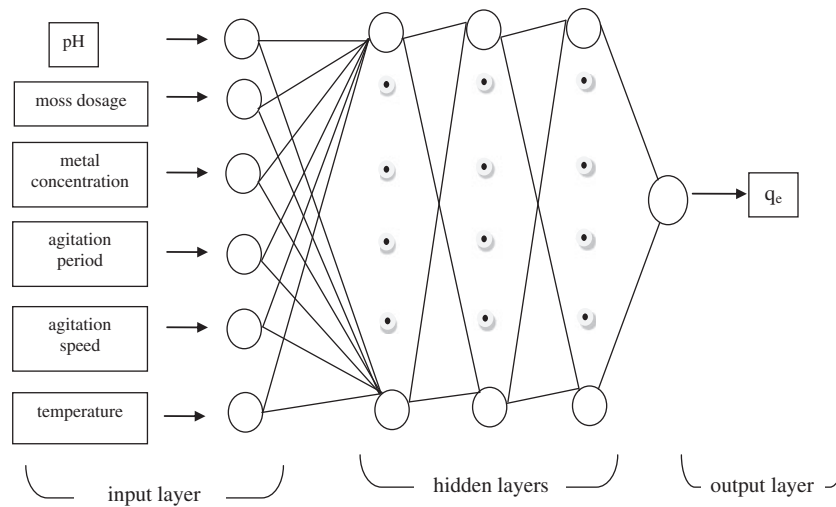
Fig. 1. Scheme of the used MLP model with three hidden layers.

sites [19,20]. The model can be expressed by the following linear equation:

$$\frac{C_e}{q_q} = \frac{1}{kV_m} + \frac{C_e}{V_m} \tag{3}$$

In the above equation, q_e (mg/g) denotes the equilibrium biosorption capacity, C_e represents the equilibrium concentration of the solution (mg/L), k and V_m are the equilibrium constant and monolayer capacity, respectively.

2.3.2. Freundlich isotherm equation

Freundlich model is another common empirical equation that assumes metal uptake occurs on heterogeneous surfaces by multilayer biosorption [21]. According to this model, it is supposed that adsorbed amount of the biosorbent increases with the increase in the concentration [22]. It is mathematically characterized by the heterogeneity factor of "$1/n$" and expressed as:

$$\log q_e = \log K_f + 1/n \log C_e \tag{4}$$

where K_f and n denote biosorption capacity and intensity, respectively [23]. Favorability of the biosorption can be determined considering the magnitude of $1/n$ values. $1/n$ values in the range 0–1 show favorable characteristic of the biosorption process.

2.3.3. Temkin isotherm equation

Temkin isotherm model considers the impacts of indirect adsorbate/adsorbate interactions [24]. The heat of biosorption decreases linearly in a layer as a result of these interactions and the biosorption is characterized by uniform distribution of bonding energies [25].

Linear form of Temkin isotherm can be expressed as:

$$q_e = B \ln A + B \ln C_e \tag{5}$$

In Eq. (5), A is the Temkin constant explaining adsorbate–adsorbate interactions and B is another constant used to explain biosorption heat.

2.4. The used kinetic models

Kinetics of heavy metal biosorption can be modeled by applying pseudo-first- and pseudo-second-order reaction kinetics [26].

2.4.1. Pseudo-first-order model

The following linear equation can be used to develop pseudo-first-order kinetic model:

$$\ln (q_e - q_t) = \ln q_e - k_1 t \tag{6}$$

In the equation, k_1 denotes the rate constant of the first-order reaction kinetic whereas q_e and q_t represent

the amount of biosorbed metal at time t and saturation (mg/g), respectively [19].

2.4.2. Pseudo-second-order model

The pseudo-second-order kinetic can be expressed by the following equation:

$$\frac{t}{q_t} = \frac{1}{k_2 q_e^2} + \frac{t}{q_e} \tag{7}$$

where k_2 denotes the rate constant of the second-order reaction kinetic.

2.5. Thermodynamic studies

Thermodynamic calculations can be performed in order to examine the feasibility of the biosorption processes. With this aim, firstly, equilibrium constant (K_c) is calculated using the following expression [15]:

$$K_c = \frac{C_{bios}}{C_e} \tag{8}$$

where C_{bios} is the amount of biosorbed metal at equilibrium (mg/g) and C_e is the equilibrium metal concentration (mg/L).

Free energy change (ΔG) can be calculated using ln K_c values as:

$$\Delta G = -RT \ln K_c \tag{9}$$

ΔG can also be expressed as:

$$\Delta G = \Delta H - T \Delta S \tag{10}$$

where ΔS and ΔH denote the entropy change and isosteric enthalpy change, respectively [25]. And finally, ln K_c can be expressed as:

$$\ln K_c = \frac{\Delta S}{R} - \frac{\Delta H}{RT} \tag{11}$$

2.6. Performance indices

Performances of the used models were evaluated using mean standard error value (MSE) and Pearson's determination coefficient (R^2) calculated according to Eqs. (12) and (13), respectively:

$$MSE = \frac{1}{N} \sum_{i=1}^{n} \left(q_{e,predict} - q_{e,exp} \right)^2 \tag{12}$$

$$R^2 = \frac{\left[\sum_{i=1}^{n} \left(q_{e,predict} - \bar{q}_{e,predict} \right) \left(q_{e,exp} - \bar{q}_{e,exp} \right) \right]^2}{\sum_{i=1}^{n} \left(q_{e,predict} - \bar{q}_{e,predict} \right)^2 \sum_{i=1}^{n} \left(q_{e,exp} - \bar{q}_{e,exp} \right)^2} \tag{13}$$

In the equations, $q_{e,predict}$ and $q_{e,exp}$ are the predicted and experimental q_e values, respectively, and $\bar{q}_e$ shows the average value of relevant q_e. $i : 1 \rightarrow n$, n is the total number of observations [15].

3. Results and discussion

3.1. Results of the characterization studies

SEM analyses were performed in order to investigate the surface area and structure morphologies of the used biosorbent. SEM images, which were taken before and after nickel biosorption have been presented in Fig. 2 (a) and (b), respectively.

Pores present on the surface of the native moss (Fig. 2 (a)) have been filled with nickel ions after biosorption process (Fig. 2 (b)).

The C, H, and N elemental analysis of the used biosorbent was found as 34.50, 4.67, and 1.22%, respectively.

The possible functional groups on moss surface were also investigated by FTIR analyses. Obtained results were given in Table 1.

As seen from Table 1, the peaks at 3429.6 and 3427.6 cm^{-1} may attribute to N–H and O–H stretching and show the presence of amines and hydroxyl groups. The peaks at 2920.5 and 2919.4 cm^{-1} are the indicators of alkyl chains–CH stretching vibration [27]. Functional groups with double bonds such as C=C, C=O, and C=N may be presented by the peaks at 1633.4 and 1631.6 cm^{-1}. Bandwidths of 1,350–1,480 cm^{-1} could be assigned to saturated alkanes and alkyl groups (R–C–H).

3.2. Experimental results

Impacts of experimental conditions were investigated by the performed batch biosorption tests. Optimum conditions were examined for pH, mass dosage, metal concentration, agitation period, agitation speed, and temperature. Obtained results have been given in terms of q_e and calculated q_e values were used for modeling purposes.
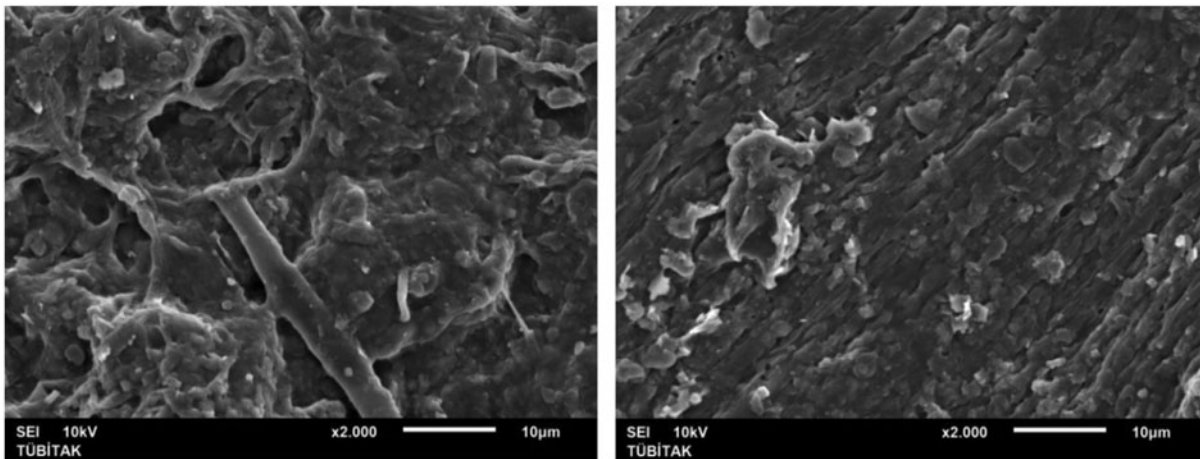
Fig. 2. SEM images of the biosorbent (a) before and (b) after nickel biosorption.

Table 1
Functional groups in native and metal loaded biosorbent

Frequency (cm^{-1})		Functional group
Native biosorbent	Loaded biosorbent	
3429.6	3427.6	N–H, O–H
2920.5	2919.4	C–H
1633.4	1631.6	C=C, C=O, C=N, R–N–H
1426.7	1426.9	R–C–H
1373.6	1373.7	R–C–H, C–O, C–N
1248.2	1250.6	C–O, C–N
1032.7	1033.9	C–O, C–N
1000–680	1000–680	R–C–H

3.2.1. Effect of pH

In the experimental studies, firstly, impacts of pH were examined as pH of the solution generally plays major role in biosorption process. In order to determine the optimum pH, 100 mL of nickel solution with 100 mg/L concentration was agitated for 90 min at 200 rpm. Biosorbent dosage was kept constant as 0.4 g. Obtained results were presented in Fig. 3.

Neutral pH levels were found to be ideal for biosorption of nickel ions by terrestrial moss, so pH 7 was determined to be optimum. At higher pH values, metal hydroxyl species may participate in the solution [28] and biosorption efficiency cannot be determined accurately due to precipitation of nickel hydroxyl ions.

3.2.2. Effect of moss dosage

Biosorbent dosage also affects the obtained biosorption efficiencies. Generally, higher biosorbent
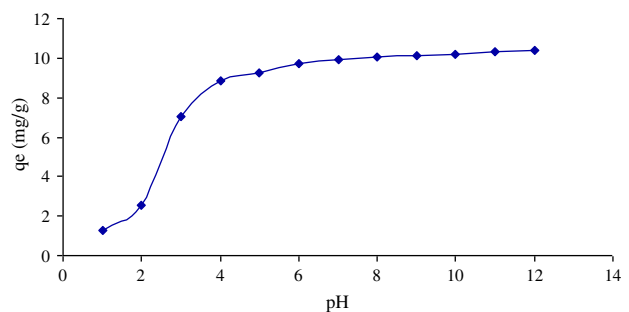

Fig. 3. Effect of pH on the biosorption of nickel by terrestrial moss. (Moss dosage 0.4 g/100 mL, nickel concentration 100 mg/L, agitation speed 200 rpm, agitation period 90 min and temperature 23°C)

dosages provide higher removal efficiency as increase in biosorbent amount yields more biosorption surface and more binding sites [29]. On the other hand, excessive biosorbent dosage may cause unsaturation

of biosorption sites. In addition, used biosorbents may aggregate in the solution. Therefore, determination of optimum biosorbent dosage is obligatory in biosorption studies.

In this study, impact of biosorbent dosage was investigated using various moss amounts in the range 0.02–1 g and optimum value was determined to be 0.6 g (Fig. 4).

3.2.3. Effect of metal concentration

Impacts of initial metal concentration were also investigated in the study. Obtained q_e values for different metal concentrations between 20 and 180 mg/L were presented in Fig. 5.

Increasing metal concentrations caused remarkable decrease in biosorption efficiency. This can be explained by the saturation of active biosorption sites by increasing concentrations. Optimum nickel concentration was determined to be 40 mg/L in this study.

3.2.4. Effect of agitation period

Batch biosorption tests were performed under predetermined optimum conditions in order to examine the optimum agitation period. In general, biosorption efficiencies tend to increase by the progress of time while the adsorbed solute tends to desorb into the solution. Finally, the system reaches equilibrium and biosorption process becomes stable [30].

In the study, impacts of agitation time were investigated for three different metal concentrations (20, 40, and 60 mg/L) and ideal agitation period was found to be 60 min for optimum nickel concentration of 40 mg/L (Fig. 6).
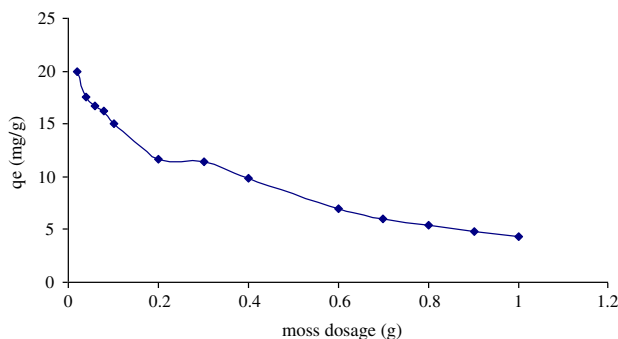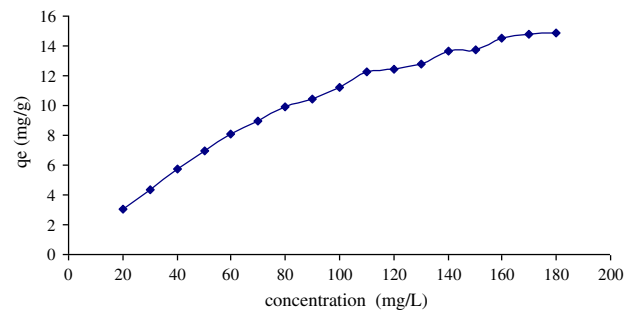
Fig. 5. Effect of metal concentration on the biosorption of nickel by terrestrial moss. (pH 7, moss dosage 0.6 g/100 mg/L, agitation speed 200 rpm, agitation period 90 min and temperature 23℃)
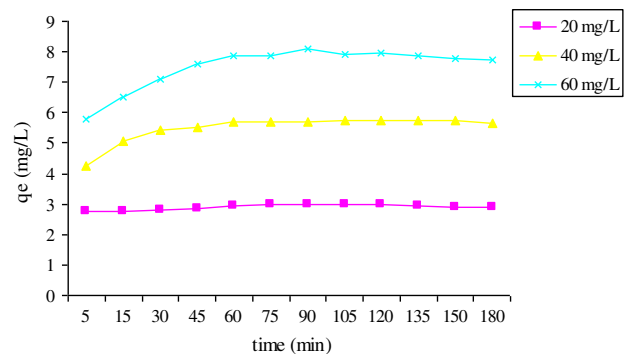
Fig. 6. Effect of agitation period on the biosorption of nickel by terrestrial moss. (pH 7, moss dosage 0.6 g/100 mg/L, nickel concentration 40 mg/L, agitation speed 200 rpm and temperature 23℃)

3.2.5. Effect of agitation speed

Agitation speed is also worth to study in biosorption process, as it has a remarkable influence on distribution of adsorbate in the solution. Impacts of various agitation speeds were presented in Fig. 7.

As seen from Fig. 7, agitation speed of 200 rpm was determined to be optimum.

3.2.6. Effect of temperature

Finally, impacts of temperature were studied by adjusting the shaking water bath to different temperature values ranging between 20 and 60℃. Increase in temperature values caused decrease in biosorption efficiency demonstrating exothermic nature of this biosorption process (Fig. 8). 20℃ was found to be optimum for the study.

Fig. 4. Effect of moss dosage on the biosorption of nickel by terrestrial moss. (pH 7, nickel concentration 100 mg/L, agitation speed 200 rpm, agitation period 90 min and temperature 23℃)
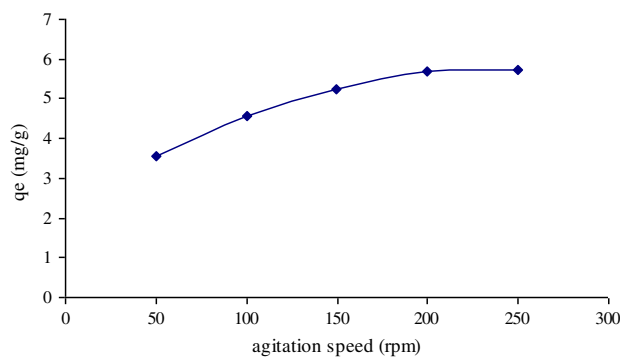
Fig. 7. Effect of agitation speed on the biosorption of nickel by terrestrial moss. (pH 7, moss dosage 0.6 g/100 mg/L, nickel concentration 40 mg/L, agitation period 60 min and temperature 23°C)
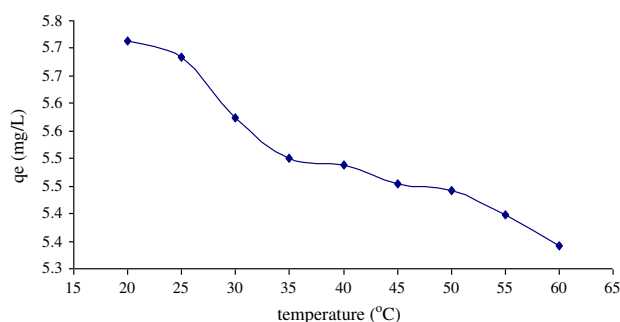

Fig. 8. Effect of temperature on the biosorption of nickel by terrestrial moss. (pH 7, moss dosage 0.6 g/100 mg/L, nickel concentration 40 mg/L, agitation period 60 min and agitation speed 200 rpm)

3.3. Results of thermodynamic analyses

In thermodynamic analyses, entropy change and isosteric enthalpy change were determined from the slope and intercept of Van't Hoff plot between $\ln K_c$ vs. $1/T$, respectively (Fig. 9).
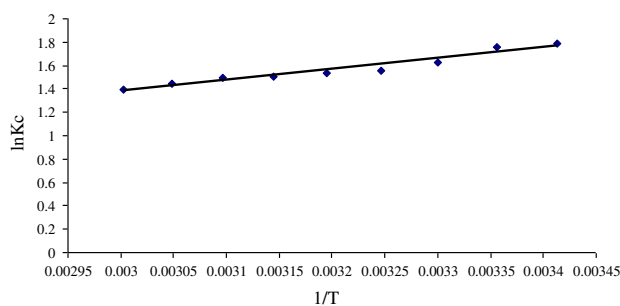

Fig. 9. Van't Hoff plot for biosorption of nickel by terrestrial moss. (pH 7, moss dosage 0.6 g/100 mg/L, nickel concentration 40 mg/L, agitation period 60 min and agitation speed 200 rpm)

Determined ΔG, ΔH, and ΔS values were given in Table 2. Negative ΔG and ΔH values indicated the spontaneous and exothermic characteristics of the biosorption process, respectively. The magnitude of ΔH provides information on the type of biosorption. ΔH values in the range 2.1–20.9 kJ/mol correspond physical biosorption whereas the values in the range 20.9–418.4 kJ/mol signify chemical biosorption [1]. In the study, ΔH value was determined as −7.72 kJ/mol and this value showed the physical nature of the biosorption process. Furthermore, negative ΔS value demonstrated the regularity of solute molecules in the biosorption [25].

3.4. Results of desorption and regeneration studies

Deionized water and nitric acid were used desorb nickel ions loaded on the used biosorbent. Desorption tests were performed in different time intervals in order to determine impact of agitation period. The percentage of ion desorbed from biomass to that biosorbed on biomass was used to evaluate the effectiveness of the elutants. Obtained results were presented in Fig. 10.

As seen from Fig. 10, HNO₃ was an effective elutant for desorption of nickel ions from the biosorbent whereas deionized water was not found to be effective. Results of the performed desorption experiments also showed that a significant desorption ratio was obtained within the first 60 min agitation period and then desorption process reached equilibrium (Fig. 10).

Regeneration process has only been performed by the biomass from which metal ions were eluated by HNO₃ as deionized water has not provided sufficient elution efficiency.

As mentioned before, three biosorption–elution–regeneration cycles were carried out in order to evaluate the reusability of the biosorbent. Nickel biosorption efficiencies were determined as 75, 60, and 40%, respectively, for the consecutive cycles whereas the raw biomass provided 87% biosorption efficiency in the first usage.

3.5. Results of the MLP models

All of the experimental data (total 86 data sets) were used in MLP modeling studies. Fifty-eight data were used for training purposes while remaining 28 data were used for testing. In training process, all of the studied factors (pH, moss dosage, metal concentration, agitation period, agitation speed, and temperature) were decided to be input parameters whereas obtained q_e values were attained as output (target) parameter. In

Table 2
Thermodynamic parameters for nickel biosorption by using terrestrial moss

Temperature (K)	ΔG (kJ/mol)	ΔH (kJ/mol)[a]	ΔS (J/molK)[a]
293	−4.36	−7.72	−11.70
298	−4.35		
303	−4.11		
308	−3.98		
313	−4.00		
318	−3.97		
323	−4.00		

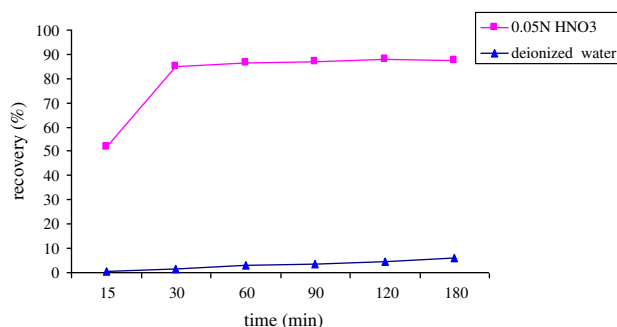[a]Measured between 293 and 333 K.

Fig. 10. The nickel desorption efficiency of the used eluants. (pH 7, moss dosage 0.6 g/100 mg/L, nickel concentration 40 mg/L, agitation speed 200 rpm and temperature 23°C)

developed models, it was aimed to obtain highest prediction efficiency by testing different training, adaptation, and learning functions. Number of hidden layers and epochs were also changed in order to achieve highest R^2 and lowest MSE values. Numerous models were developed considering these goals.

In Table 3, properties and efficiencies of some selected models were summarized. As seen from the table, architectures of the models have great impacts on the obtained prediction efficiencies. Calculated R^2 and MSE values significantly change with the changing functions.

Comparing the results of Models VII, IX, X, and XI, it is clearly seen that number of hidden layers also affect the modeling performance. Determination of ideal hidden layer number, which is also the sign of the complexity of the problem, is obligatory in MLP model studies. In general, more hidden layers are required for expression of more complex problems.

Determination of appropriate iteration number is also demanded in MLP modeling studies for achieving sufficient learning performance. The network cannot learn efficiently if epoch number is inadequate, on the

other hand, the model memorizes the results in case of excessive epochs. This fact explains the results of Models V, VI, VII, and VIII.

In the study, highest modeling efficiency was obtained with Model X, which uses TRAINR learning function, Learngdm adaptation function, and Logsig transfer function. In the developed model, three hidden layers and 4,000 epochs were used. Obtained prediction performance was explained with R^2 value of 0.90 and MSE value of 0.006 (Table 3). Experimental and predicted q_e values are shown in the graph for Model X (Fig. 11).

3.6. Results of the isotherm models

In the study, Langmuir, Freundlich, and Temkin conventional isotherm models were used to analyze equilibrium data. In Fig. 12, plots of C_e/q_e vs. C_e, $\log q_e$ vs. $\log C_e$, and q_e vs. $\ln C_e$ were presented, respectively, for Langmuir, Freundlich, and Temkin models.

As seen from the graphs presented in Fig. 12, all plots yield straight lines with adequate R^2 values. Isotherm model parameters were also calculated slopes and intercepts of these plots (Table 4).

As seen from Table 4, calculated isotherm parameters indicated the appropriateness of the applied models. Although both Langmuir and Freundlich models were found to be appropriate, the biosorption process was better represented by Freundlich equation considering higher R^2 values. This suggests heterogeneity in the surface or pores of the used biosorbent.

MSE values were also determined for all of the models. Comparatively, higher error value (1.343) was found for Temkin isotherm.

3.7. Results of the kinetic models

Pseudo-first- and pseudo-second-order reaction kinetics were used in order to explain the mechanism

Table 3
Properties and efficiencies of the selected MLP models for prediction biosorption of nickel by using terrestrial moss.

Model no.	Training function	Adaptation function	Transfer function	Number of hidden layers	Number of epochs	R^2	MSE
I	Traingdm	Learngdm	Logsig	3	3,000	0.28	0.043
II	Traingd	Learngd	Logsig	4	3,000	0.52	0.036
III	Trainlm	Learngdm	Logsig	3	3,000	0.26	0.091
IV	Trainlm	Learngd	Tansig	3	4,000	0.50	0.093
V	Trainr	Learngdm	Logsig	4	2,000	0.69	0.019
VI	Trainr	Learngdm	Logsig	4	3,000	0.78	0.019
VII	Trainr	Learngdm	Logsig	4	4,000	0.86	0.009
VIII	Trainr	Learngdm	Logsig	4	5,000	0.59	0.059
IX	Trainr	Learngdm	Logsig	5	4,000	0.68	0.034
X	**Trainr**	**Learngdm**	**Logsig**	**3**	**4,000**	**0.90**	**0.006**
XI	Trainr	Learngdm	Logsig	2	4,000	0.84	0.016
XII	Trainr	Learngdm	Tansig	3	4,000	0.74	0.043
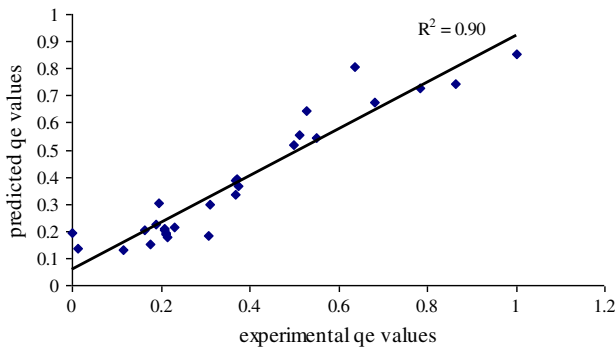
Fig. 11. Experimental and predicted q_e values obtained with MLP model.

and characteristics of the biosorption process [17]. Plots of $\ln(q_e - q_t)$ against time and t/q_t against time were presented, respectively, for pseudo-first- and pseudo-second-order kinetic models in Fig. 13.

As seen from Fig. 13 (a) and (b), curves in plots are linear. Rate constants (k_1 and k_2) and $q_{e,calculated}$ values were determined from the slopes and intersection points of these curves for all the tested metal concentrations.

All calculated kinetic parameters for pseudo-first- and pseudo-second-order reaction kinetics were presented in Table 5. As seen from Table 5, $q_{e,calculated}$ and $q_{e,experimental}$ values were remarkably closer in pseudo-second-order reaction kinetics. Furthermore, determined correlation coefficients were higher for second-order reaction kinetics.

If efficiencies of MLP models, isotherm, and kinetic models are evaluated together, it is clearly seen that all models provide remarkable modeling performances
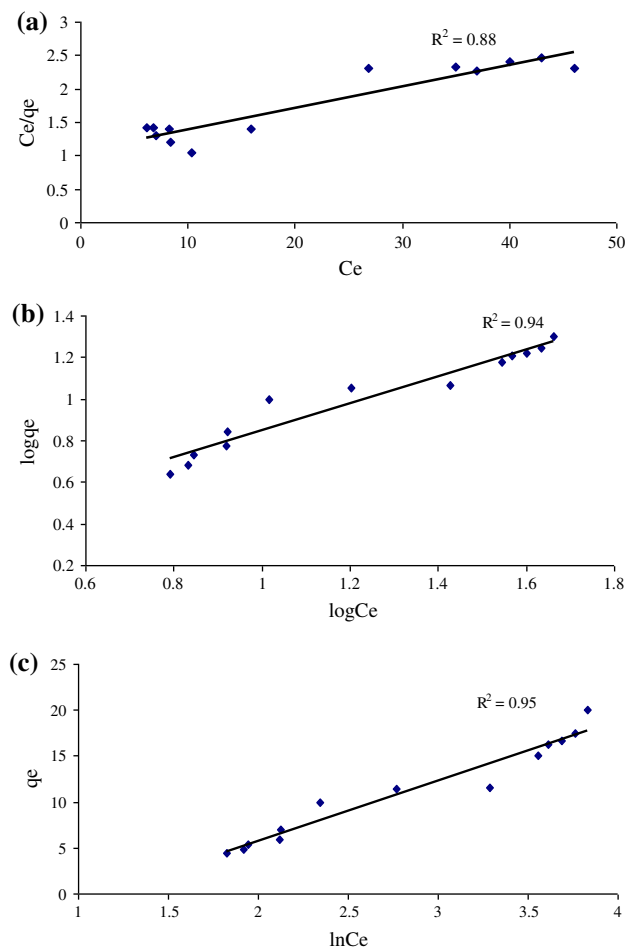

Fig. 12. Langmuir (a), Freundlich (b) and Temkin (c) isotherm models for the biosorption of nickel by using terrestrial moss.

Table 4
Calculated isotherm parameters for biosorption of nickel by using terrestrial moss

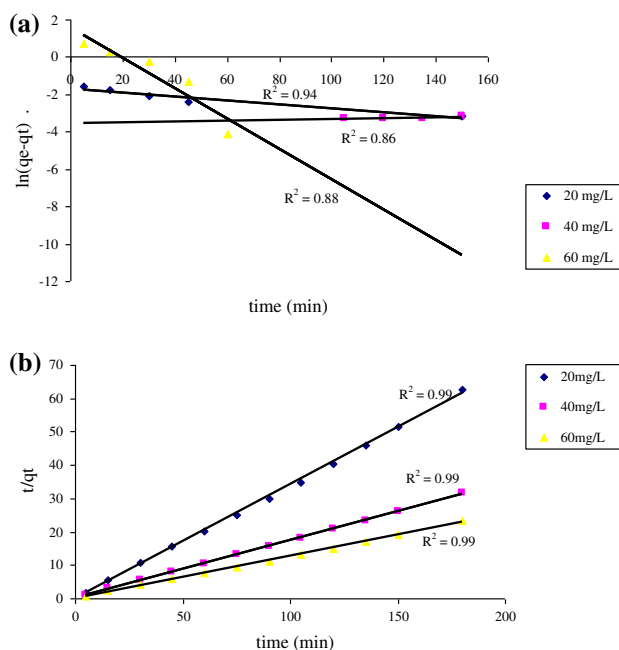| Langmuir				Freundlich				Temkin			
Vm	k	R^2	MSE	K_f	$1/n$	R^2	MSE	A	B	R^2	MSE
31.25	0.03	0.88	0.034	4.44	0.64	0.94	0.003	0.324	6.57	0.95	1.343

Fig. 13. Pseudo-first- (a) and pseudo-second-order (b) reaction kinetics for the biosorption of nickel by using terrestrial moss.

to explain the biosorption of nickel ions using terrestrial moss. Most important superiority of the MLP models is to yield predictions considering all effective factors (pH, moss dosage, initial metal concentration, agitation period, agitation speed, and temperature) together at the same time. This provides more realistic and accurate information about the biosorption

processes which are affected by numerous factors simultaneously. On the other hand, conventional isotherm and kinetic models explain biosorption phenomenon considering the equilibrium and kinetic data, respectively. So, results obtained from these conventional models explain more specific conditions.

Conclusions

The aim of this work was to investigate efficiencies of MLP models and conventional isotherm equations for modeling biosorption behaviors of nickel using terrestrial moss. With this aim, batch biosorption tests were performed under different experimental conditions. Obtained experimental data were used to run the models. Performed thermodynamic studies showed that the biosorption process exhibits spontaneous and exothermic characteristics.

In the study, performance of the MLP models was evaluated using calculated R^2 and MSE values. Isotherm parameters, R^2, and MSE values were determined to examine the appropriateness of the isotherm models whereas kinetic parameters, R^2, and MSE values were used to evaluate the appropriateness of kinetic models.

In MLP modeling studies, obtained results showed that architecture of the developed model was very effective on the prediction performances. Selection of appropriate functions, number of hidden layers, and epochs is obligatory to obtain sufficient modeling efficiency. Among the numerous developed models, highest prediction efficiency was obtained by a backpropagation feedforward network type with three hidden layers (Model X). TRAINR learning function,

Table 5
Calculated kinetic parameters for biosorption of nickel by using terrestrial moss

Initial metal concentration (mg/L)	$q_{e,experimental}$ (mg/g)	Pseudo-first-order				Pseudo-second-order			
		k_1 (1/min)	$q_{e,calculated}$ (mg/g)	R^2	MSE	k_2 (g/mg min)	$q_{e,calculated}$ (mg/g)	R^2	MSE
20	2.94	1.05×10^{-2}	0.19	0.94	0.15	12.80×10^{-1}	2.92	0.99	0.34
40	5.70	2.60×10^{-3}	0.02	0.86	0.03	11.00×10^{-2}	5.79	0.99	0.01
60	7.86	8.15×10^{-2}	4.90	0.88	1.26	7.90×10^{-2}	7.93	0.99	0.04

Learngdm adaptation function, and Logsig transfer function were used in this ideal model. Four thousand epochs were found to be appropriate in learning process. R^2 and MSE values of the model were determined as 0.90 and 0.006, respectively.

Langmuir, Freundlich, and Temkin isotherm models were applied to equilibrium data. Obtained isotherm parameters indicate the appropriateness of these conventional models. Calculated R^2 values were found as 0.88, 0.94, and 0.95, respectively, for Langmuir, Freundlich, and Temkin isotherm models. In the study, heterogeneous biosorption model was found to be better for isotherm simulation considering the higher R^2 value obtained in Freundlich model. Calculated $1/n$ value (0.64) also indicated favorable characteristic of the biosorption process.

It can be concluded that the biosorption mechanism has followed pseudo-second-order kinetics considering higher R^2 values. Furthermore $q_{e,calculated}$ and $q_{e,experimental}$ values were found to be closer in second-order kinetic model.

Although all of the applied models were seemed to be efficient, MLP models are thought to be more useful as they make predictions using data that are more comprehensive. All effective factors (pH, biosorbent dosage, metal concentration, agitation time, etc.) were evaluated together in MLP models whereas more specific information can be obtained by conventional isotherm models. So, MLP models are thought to be representative and realistic for explaining complex biosorption process. The sole disadvantage of the models is the demand for numerous time-consuming tests performed to determine the ideal network architecture.

References

[1] A. Sari, D. Mendil, M. Tuzen, M. Soylak, Biosorption of palladium(II) from aqueous solution by moss (*Racomitrium lanuginosum*) biomass: Equilibrium, kinetic and thermodynamic studies, J. Hazard. Mater. 162 (2009) 874–879.

[2] N. Barka, K. Ouzaouit, M. Abdennouri, M.E. Makhfouk, Dried prickly pear cactus (*Opuntia ficus indica*) cladodes as a low-cost and eco-friendly biosorbent for dyes removal from aqueous solutions, J. Taiwan Inst. Chem. Eng. 44 (2013) 52–60.

[3] S.V. Mohan, S.V. Ramanaiah, B.P. Rajkumar, N. Sarma, Removal of fluoride from aqueous phase by biosorption onto algal biosorbent *Spirogyra* sp.-*IO2*: sorption mechanism elucidation, J. Hazard. Mater. 141 (2007) 465–474.

[4] I. Tüzün, G. Bayramoğlu, E. Yalçın, G. Başaran, G. Çelik, Equilibrium and kinetic studies on biosorption of Hg(II), Cd(II) and Pb(II) ions onto microalgae *Chlamydomonas reinhardtii*, J. Environ. Manage. 77 (2005) 85–92.

[5] S.V. Bhat, J.S. Melo, B.B. Chaugule, S.F.J. D'Souza, Biosorption characteristics of uranium(VI) from aqueous medium onto *Catenella repens*, a red alga, J. Hazard. Mater. 158 (2008) 628–635.

[6] W. Fan, Z. Xu, Biosorption of nickel ion by chitosan-immobilized brown algae *Laminaria japonica*, Chem. Biochem. Eng. Q. 25 (2011) 247–254.

[7] A.P. Rawat, M. Rawat, J.P. Rai, Toxic metals biosorption by *Jatropha curcas* deoiled cake: Equilibrium and kinetic studies, Water Environ. Res. 85 (2013) 733–742.

[8] J. Yu, B. Li, X. Sun, Y. Jun, Adsorption of methylene blue and rhodamine B on baker's yeast and photocatalytic regeneration of the biosorbent, Biochem. Eng. J. 45 (2009) 145–151.

[9] M.T. Uddin, M. Rukanuzzaman, M.M. Maksudur Rahman Khan, M.A.J. Akhtarul Islam, Adsorption of methylene blue from aqueous solution by jackfruit (*Artocarpus heteropyllus*) leaf powder: A fixed-bed column study, J. Environ. Manage. 90 (2009) 3443–3450.

[10] C.-H. Weng, Y.-T. Lin, T.-W. Tzeng, Removal of methylene blue from aqueous solution by adsorption onto pineapple leaf powder, J. Hazard. Mater. 170 (2009) 417–424.

[11] R. Han, Y. Wang, X. Zhao, Y. Wang, F. Xie, J. Cheng, M. Tang, Adsorption of methylene blue by phoenix tree leaf powder in a fixed-bed column: Experiments and prediction of breakthrough curves, Desalination 245 (2009) 284–297.

[12] W.S. Wan Ngah, M.A.K.M. Hanafiah, Adsorption of copper on rubber (*Hevea brasiliensis*) leaf powder: Kinetic, equilibrium and thermodynamic studies, Biochem. Eng. J. 39 (2008) 521–530.

[13] K.G. Bhattacharyya, A.J. Sharma, Adsorption of Pb(II) from aqueous solution by *Azadirachta indica* (neem) leaf powder, J. Hazard. Mater. 113 (2004) 97–109.

[14] N.G. Turan, B. Mesci, O. Ozgonenel, The use of artificial neural networks (ANN) for modeling of adsorption of Cu(II) from industrial leachate by pumice, Chem. Eng. J. 171 (2011) 1091–1097.

[15] U. Özdemir, B. Özbay, S. Veli, S. Zor, Modeling adsorption of sodium dodecyl benzene sulfonate (SDBS) onto polyaniline (PANI) by using multi linear regression and artificial neural networks, Chem. Eng. J. 178 (2011) 183–190.

[16] G.M. Smith, Cryptogamic Botany, Volume II – Bryophytes and Pteridophytes, McGraw-Hill Book Company, New York, NY, 1938.

[17] R. Gong, Y. Ding, H. Liu, Q. Chen, Z. Liu, Lead biosorption and desorption by intact and pretreated *spirulina maxima* biomass, Chemosphere 58 (2005) 125–130.

[18] B. Özbay, Modeling the effects of meteorological factors on SO$_2$ and PM10 concentrations with statistical approaches, Clean—Soil Air Water 40 (2012) 571–577.

[19] B. Alyüz, S. Veli, Kinetics and equilibrium studies for the removal of nickel and zinc from aqueous solutions by ion exchange resins, J. Hazard. Mater. 167 (2009) 482–488.

[20] Z. Li, T.T. Teng, A.F.M. Alkarkhi, M. Rafatullah, L.W. Low, Chemical modification of *Imperata cylindrica* leaf powder for heavy metal ion adsorption, Water Air Soil Pollut. 224 (2013) 1505–1518.

[21] M. Liu, H. Zhang, X. Zhang, Y. Deng, W. Liu, H. Zhan, Removal and recovery of Chromium(III) from aqueous solutions by a spheroidal cellulose adsorbent, Water Environ. Res. 73 (2001) 322–328.

[22] S. Babel, T.A. Kurniawan, Removal from synthetic wastewater using coconut shell charcoal and commercial activated carbon modified with oxidizing agents and/or chitosan, Chemosphere 54 (2004) 951–967.

[23] V. Chantawong, N.W. Harvey, V.N. Bashkin, Comparison of heavy metal adsorptions by Thai kaolin and ballclay, Water Air Soil Pollut. 148 (2003) 111–125.

[24] H. Zheng, D. Liu, Y. Zheng, S. Liang, Z. Liu, Sorption isotherm and kinetic modeling of aniline on Cr-bentonite, J. Hazard. Mater. 167 (2009) 141–147.

[25] İ. Özbay, U. Özdemir, B. Özbay, S. Veli, Kinetic, thermodynamic, and equilibrium studies for adsorption of azo reactive dye onto a novel waste adsorbent: Charcoal ash, Desalin. Water Treat. 51 (2013) 6091–6100.

[26] A. Kapoor, T. Viraraghavan, D. Roy Cullimore, Removal of heavy metals using the fungus *Aspergillus niger*, Bioresour. Technol. 70 (1999) 95–104.

[27] J. Pan, R. Liu, H. Tang, Surface reaction of *Bacillus cereus* biomass and its biosorption for lead and copper ions, J. Environ. Sci. 19 (2007) 403–408.

[28] A. Kaya, A.H. Ören, Adsorption of zinc from aqueous solutions to bentonite, J. Hazard. Mater. 125 (2005) 183–189.

[29] A. Adak, M. Bandyopadhyay, A. Pal, Removal of crystal violet dye from wastewater by surfactant-modified alumina, Sep. Purif. Technol. 44 (2005) 139–144.

[30] W.S. Ngah, S. Fatinathan, Pb(II) biosorption using chitosan and chitosan derivatives beads: Equilibrium, ion exchange and mechanism studies, J. Environ. Sci. 22 (2010) 338–346.